Philiadium Gregarum versus *Aurelia aurita*: on propulsion efficiency in jellyfish

S. Etienne*, A. Garon†, D. Pelletier‡
École Polytechnique de Montréal, C.P. 6079, succ. Centre-ville, Montréal, Québec, H3C 3A7, Canada
C. Cameron§
Université de Montréal, Montréal, Québec, Canada

Abstract

A Fluid-Structure Finite Element Method is developed to compare the self propulsion mechanism efficiency of two jellyfishes, *Philiadium Gregarum* and *Aurelia aurita*. The motion is generated by circular muscles that contract and generate a hydrodynamic propulsive jet. This jet is the principal source of thrust of jellyfishes. The propulsive efficiency of the animal can be evaluated when comparing the resulting momentum with input power from the muscles. An axisymmetric numerical model of the animal has been set up and muscular forces modeled by body forces. Several parameters control this Fluid-Structure configuration. For instance, the excitation forces of muscles over a propulsive cycle, shape, amplitude, frequency, contraction, relaxation, the material properties and the morphology of the jellyfish body are key parameters.

I. Introduction

Biology offers a wide variety of propulsive mechanisms that engineers can mimic to their advantage.[1,2] In hydrodynamics, cetaceans have evolved shapes that delay stall on their flippers thus enhancing both manoeuvering and propulsive efficiency.[3] The case of the jellyfish, is especially interesting because the mechanism for its propulsion is very different from that of whales. The cyclic contractions of its bell result in a sequence of periodic impulse jets. Several experimental studies describe the kinematics and dynamics of the motion from video recordings and wake measurements.[4–6]

Dabiry[5] studied the swimming performance of jellyfish from a vortex dynamics point of view. More precisely, they studied the properties of the wake induced by the motion of the animal. They show that the vortex ring generated by jetting contributes to the propulsive forces in terms of vortex added-mass. Hence it contributes to the regulation of the body motion of the animal over one cycle. Peng and Dabiri[6] applied the Lagrangian Coherent Structures approach in a potential flow to deduce forces and moments on a swimming animal.

McHenry and Jed[4] studied the hydrodynamic and swimming performance of an *Aurelia Aurita*. They develop a point mass model based on Newton's first law of dynamics, correlations for forces and some kinematic information extracted from video recordings in the wild. The model was calibrated on other video data. They used this calibrated model to understand the scaling rules for hydrodynamic forces and predict how changes in size, shape and motion of the body influence the swimming performance. Their conclusion is that shape is very important. Prolateness of the bell controls the energetic cost of motion and the speed. The more prolate the bell is, the faster the jellyfish swims and the more energy it consumes. The model relies so much on correlation that they experience difficulties at discriminating between slightly different individuals. Achieving such level of resolution requires higher fidelity models capable of describing the details of the flow

*Researcher, Département de Génie Mécanique
†Professor, Département de Génie Mécanique
‡Canada Research Chair, Département de Génie Mécanique, Associate Fellow AIAA
§Professor, Département de Sciences Biologiques

in and around the medusa, and the large displacements and geometrical changes of the bell. This is the topic of our paper.

The fourth author of this abstract harvested samples of the population *Philiadium Gregarum* in the coastal water of British-Columbia during the month of June 2008. He measured the geometrical characteristics of individual of different sizes (equivalent to age).

From available data in the literature on *Aurelia Aurita* and our data on *Philiadium Gregarum* we can compare the efficiency of both jellyfishes.

We use the partial differential equations describing viscous laminar flows (the Navier-Stokes equations) and nonlinear equations of hyperelasticity to predict the forces and moments that enter the equations describing the dynamics of the motion of the medusa's center of mass. (*i.e.* the correlations of the previous models)

Zhao *et al.* applied a cartesian mesh method combined to a projection technique and computed a swimming period of a jellyfish in two-dimensions. An advantage of this combined method is that deformation of the mesh is not an issue. However, the immersed-interface treatment requiring projection and the interpolation of the different variables at the interface location both affect the overall accuracy.

We here study the jellyfish motion in an axisymmetric frame of reference with an ALE-FEM formulation for the incompressible fluid flow and a Total Lagrangian FEM formulation for the solid. We first present the governing equations and the solution procedure and then show results for a jellyfish motion.

II. Shapes of the two species

The typical shapes of the *Philiadium Gregarum* and *Aurelia Aurita* jellyfishes are shown on Fig. 1. Data concerning *Philiadium Gregarum* have been obtained on samples collected by Chris Cameron off the coast of Vancouver Island. Geometrical shapes as well as density of the animals have been measured. Period of motion, amplitudes of bell displacements, forward velocities and periods of contraction have been recorded on these samples. Informations for *Aurelia Aurita* have been extracted from the work by McHenry and Jed.[4]

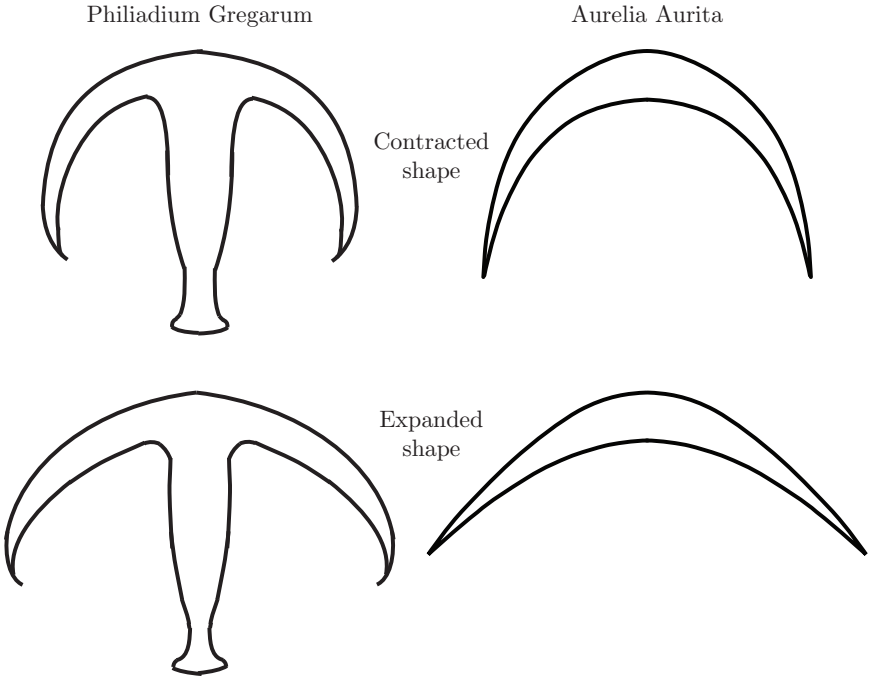

Figure 1. Shapes of *Philiadium Gregarum* and *Aurelia Aurita*.

III. Governing Equations

The flow of an incompressible fluid is described by the continuity and momentum equations[7] written in *convective* (non-conservative) form

$$\boldsymbol{\nabla} \cdot \mathbf{u}_f = 0 \tag{1}$$

$$\rho_f \mathbf{u}_{f,t} + \rho_f \mathbf{u}_f \cdot \boldsymbol{\nabla} \mathbf{u}_f = \boldsymbol{\nabla} \cdot \boldsymbol{\sigma}_f \tag{2}$$

On an arbitrary time-dependent coordinate system, the momentum equations (2) are written as ([8])

$$\rho_f \mathbf{u}_{f,t} + \rho_f (\mathbf{u}_f - \mathbf{u}_m) \cdot \boldsymbol{\nabla} \boldsymbol{u} = \boldsymbol{\nabla} \cdot \boldsymbol{\sigma}_f \tag{3}$$

where $\mathbf{u}_m$ is the mesh velocity, ρ_f the fluid density, $\mathbf{u}_f$ the fluid velocity, $\boldsymbol{\sigma}_f$ the total fluid stress tensor (pressure and viscous forces). Equations (1) and (2) are expressed in an Eulerian frame of reference while equation (3) is expressed in an Arbitrary Lagrangian Eulerian (ALE) coordinate system. Details of its development can be found in the paper by Lacroix and Garon.[8] Assuming that the fluid is Newtonian, its constitutive equation is given by:

$$\begin{aligned} \boldsymbol{\sigma}_f &= \boldsymbol{\tau}_f - p\mathbf{I} \\ &= \mu_f [\boldsymbol{\nabla} \mathbf{u}_f + (\boldsymbol{\nabla} \mathbf{u}_f)^T] - p\mathbf{I} \end{aligned}$$

where μ_f is the dynamic viscosity and p is the fluid pressure. The flow equations are closed with the following boundary conditions,

$$\begin{aligned} \boldsymbol{\sigma}_f \cdot \mathbf{n} &= \overline{\mathbf{t}}_f && \text{on } \Gamma_N^f \\ \mathbf{u}_f &= \overline{\mathbf{u}}_f && \text{on } \Gamma_D^f \end{aligned} \tag{4}$$

where Γ_N^f denotes a boundary where Neumann conditions are applied in the form of prescribed surface forces (tractions) $\overline{\mathbf{t}}_f$, and Γ_D^f corresponds to a Dirichlet boundary on which the velocity, $\overline{\mathbf{u}}_f$, is imposed.

The differential equations for equilibrium on the initial undeformed configuration are

$$\begin{aligned} \rho_{s0} \mathbf{u}_{s,t} + \nabla \cdot \boldsymbol{\sigma}_l + \mathbf{f}_s &= 0 \\ \mathbf{u}_s &= \boldsymbol{\chi}_{s,t} \end{aligned} \tag{5}$$

with $\mathbf{f}_s$ a body force.

$$\boldsymbol{\sigma}_l = \mathbf{F} \boldsymbol{\sigma}_k \tag{6}$$

$$\boldsymbol{\sigma}_k = \lambda_s tr(\mathbf{E}) \mathbf{I} + 2\mu_s \mathbf{E} \tag{7}$$

where λ_s and μ_s are the Lamé constants and $\mathbf{E}$ the Green-Lagrange strain tensor.

Eqs. (5) are supplemented by the following boundary conditions,

$$\boldsymbol{\sigma}_l \cdot \mathbf{n} = \overline{\mathbf{t}}_s \qquad \text{on } \Gamma_N^s \tag{8}$$

$$\boldsymbol{\chi}_s = \overline{\boldsymbol{\chi}_s} \qquad \text{on } \Gamma_D^s \tag{9}$$

Along the fluid-solid interface one must have

$$\mathbf{u}_f = \mathbf{u}_s \tag{10}$$

$$\boldsymbol{\sigma}_c \hat{\mathbf{n}}_s + \boldsymbol{\sigma}_f \hat{\mathbf{n}}_f = 0 \tag{11}$$

where $\boldsymbol{\sigma}_s$ is the Cauchy stress tensor and $\boldsymbol{\sigma}_f$ is the usual viscous stress tensor.

$$\boldsymbol{\sigma}_c = \frac{\mathbf{F} \boldsymbol{\sigma}_k \mathbf{F}^T}{J} \tag{12}$$

$$\tag{13}$$

IV. Motion of the mesh

The mesh motion is arbitrary except on the solid-fluid interface where the fluid nodes and solid nodes must follow the interface distortion and motion. Our ALE formulation is adapted for describing the fluid flow in a deforming domain and the motion of the fluid mesh is described by linear elasticity equations, the so-called pseudo-solid approach.[9] In this approach, the fluid domain is assumed to deform like an elastic solid body so that the usual Lagrangian elasticity equations of solid mechanics can be used to ensure that the shape of the fluid domain conforms to the new geometry of the animal.

V. Motion of the interface nodes

If the initial boundary discretisation resolves nicely the surface of the animal, interface nodes need not move in the tangential direction, *i.e.* they stick to the animal surface.

VI. Key components of the simulation

A successful simulation of the propulsion of a jellyfish must simultaneously account for

1. the details of the hydrodynamic forces on the jellyfish and the details of the flow in and around the animal,
2. the large finite displacements of the bell of the jellyfish causing the pulsatile jetting action responsible for its motion,
3. the motion of the animal in an inertial frame of reference.

These steps are accounted for by the PDE's described in the previous section

VII. Finite element solver

A monolithic formulation of the above equations is adopted. It couples all degrees of freedom of the problem:

- velocity, pressure and pseudo-solid displacements in the fluid domain (u, v, p, ξ, η)
- velocity and displacements in the solid (u, v, ξ, η)
- reactions at the interface.

This approach requires that all equations be treated implicitly in the time integration scheme. This methodology is applicable not only for flows on deforming meshes but also to fully implicit monolithic treatment of unsteady Fluid-Structure Interactions. Linearization of the flow and mesh equations must account for all implicit dependencies to ensure quadratic convergence of Newton's method.[10] These steps are implemented in a simple and straightforward manner through the use of a numerical Jacobian.

The velocity and displacement fields are discretized using 6-noded quadratic elements. Fluid pressure is discretized by piecewise linear continuous functions. The resulting sparse matrix system is solved using the PARDISO software.[11,12]

The temporal ans spatial accuracy of the monolithic FSI algorithm has been verified in previous communications.[13,14]

VIII. Preliminary Numerical results

The geometry and boundary conditions are depicted on Fig. 2. Except for boundary conditions on the symmetry axis and interface between fluid and solid, all boundary conditions are Neumann boundary conditions. This allows the domain to move along with the animal. The non-dimensional Young modulus of the solid is 130, its Poisson coefficient is 0.45. The non-dimensional fluid viscosity is 2.10^{-4}, the non-dimensional fluid density is equal to 1 as is that of the jellyfish. The system is started from rest and body forces are applied periodically to mimic the stress of the jellyfish muscles as depicted on Fig. 3.

The muscle excitation of the jellyfishes are of pacemaker type so that a periodic excitation corresponds well to the natural behavior of these animals. The non-dimensional period is $T = 15$. We have chosen the force time evolution described on Fig. 3. The direction is transverse to the motion of the animal since muscles are axisymmetric and thus can only contract radially. It is difficult to obtain data on the excitation of muscles. However, McHenry[4] described cycles of the motion of jellyfishes and observed that excitation takes place over a quarter of a period while the other three-quarters correspond to relaxation.

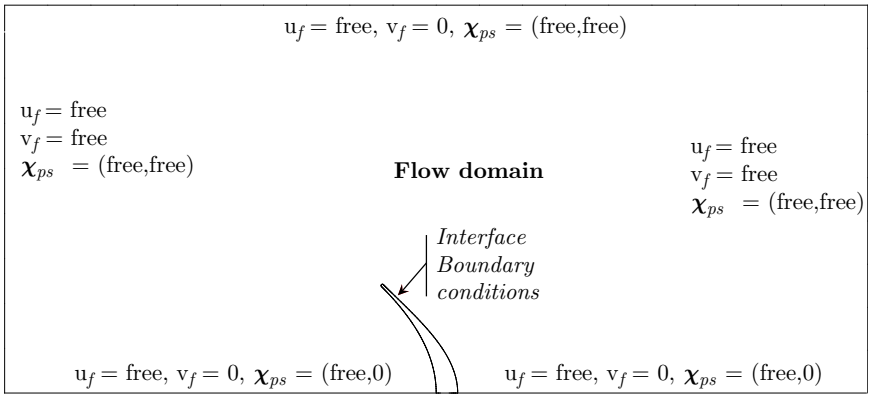

Figure 2. Geometry and boundary conditions for the jellyfish FSI problem.

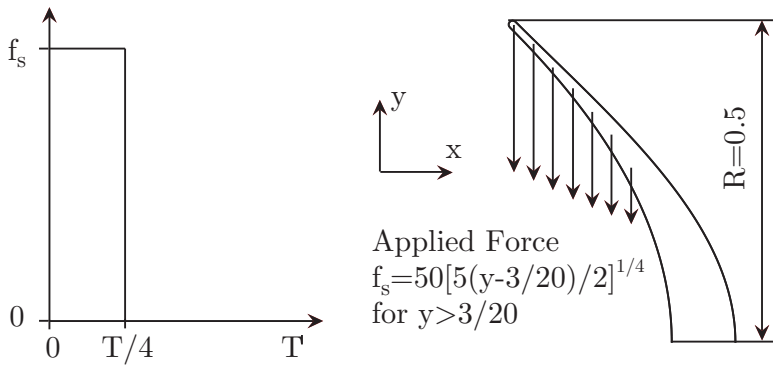

Figure 3. Direction and intensity of the force model representing the jellyfish muscles.

The mesh used for the simulation is depicted on figure 4. It is constituted of 96000 nodes and 48000 elements. There are two levels of node concentration. The most visible is the one corresponding to the near wake generated by the animal. An additional level of mesh refinement is required around the tip of the bell. This is necessary to properly resolve the large shear strains and pressure gradients occurring in this area.

Figure 5 shows the vorticity field at different instants in a cycle. Note that vorticity always remain positive inside the bell. This confers two properties. Firstly, vorticity naturally brings nutrients to the mouth. Secondly, it contributes to the motion of the animal since it brings fluid inside the umbrella which maintains a high pressure level. Note that negative vortex rings are ejected in the wake. Their effects on motion decays quickly with distance.

Referring to Fig. 6, the interval from t=0 to 30 corresponds to the initial transient in which the animal accelerates from rest over two periods of contraction. Beginning with t=30 the jellyfish appears to have reached an established pulsed motion. During the third period of simulation t=30 to 45, the animal has moved by 1.5 diameter which appears to be in agreement with experimental observations.[4,15]

Note the large displacements of the tip of the bell at $t = 32.5$ (the maximum occurs at the end of the contraction (1/4 period) at $t = 33.5$. This a clear indication that the structural model of the jellyfish bell must at the very least include geometric nonlinearities. given that the jellyfish is mostly water, it is possible that a constitutive equation for incompressible material might also be required.

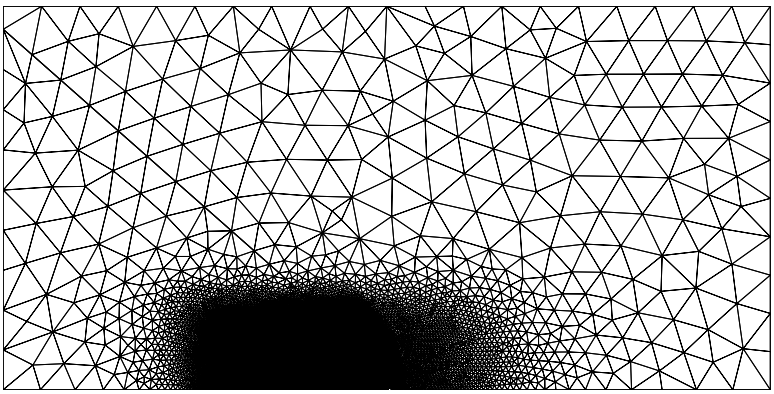

Figure 4. Mesh of 96000 nodes.

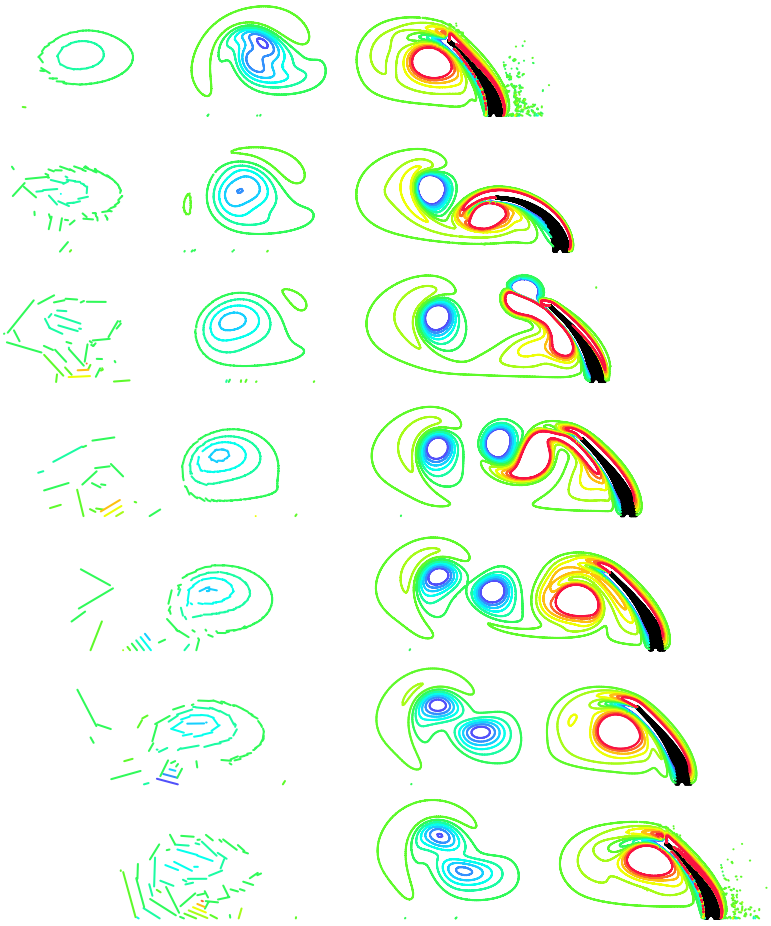

Figure 5. Vorticity field and jellyfish shape at t =30, 32.5, 35, 37.5, 40., 42.5, 45.

We can convert dimensionless results to dimensional responses. Noting that viscosity of sea water is $10^{-6}m^2/s$ and that our non-dimensional viscosity is set to 2.10^{-4}, we find that our model corresponds to medusa with a diameter of $2cm$ and of a period of $1.2s$. With this information, we calculate that the animal moved by $3cm$ over the third period of Fig. 6 at a speed of $2.5cm/s$ which is in the range of observed velocities for individuals of this size.

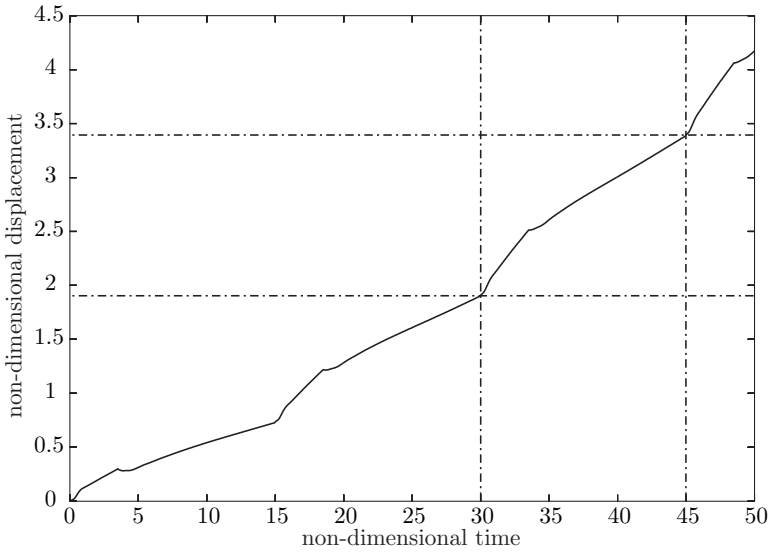

Figure 6. Displacement as a function of time.

IX. Conclusions

We have presented a flow-structure interaction model for predicting the swimming characteristics of jellyfishes. Preliminary results indicate that the predicted motion of the animal compares well with in-situ measurements.

A. Work-In-Progress

Work progresses over several fronts.

- the final manuscript will report all details on the geometry of the 2 species,
- the final manuscript will provide all data used for the simulations including density, viscosity of the fluid, material properties of the body of the animals,
- the manuscript will compare effects of stem in Philadium on propulsion and flow
- the manuscript will report details of the flow fields generated by the two species velocity, pressure, vorticity fields absolute streamlines and streak lines to document the flows around each animal,
- details of the mesh will be provided along with a description of the procedures and constraints imposed on the motion of the mesh to avoid negative volumes of elements,
- comparison will be made via solution animation,
- finally predictions will be compared to field measurements for global quantities such as displacement and speed of the center of mass of the animals, and local quantities such as velocity and vorticity fields extracted from PIV measurements performed at University of British Columbia.

Acknowledgements

This work was sponsored in part by NSERC (Government of Canada) and the Canada Research Chair Program (Government of Canada).

References

[1]D.J. Willis, E.R. Israeli, P.O. Persson, M.Drela, J. Peraire, S.M. Swartz, and K.s. Breuer. A computational framework for fluid-structure interaction in biologically inspired flapping flight. In *46th AIAA Aerospace Sciences Meeting*, Reno, NV, Jan. 2008. AIAA Paper 2008-523.

[2]W. Shyy, Y. Lian, J. Tang, H. Liu, P. Trizila2008, B. Stanford, L. Bernal, C. cesnik, P. Friedmann, and P. Ijfu. Computational aerodynamics of low reynolds nyumber plunging, pitching and flexible wings for mav applications. In *46th AIAA Aerospace Sciences Meeting*, Reno, NV, Jan. 2008. AIAA Paper 2008-523.

[3]H.T.C. Pedro and M.H. Kobayashi. Numerical study of stall delay on humpback whale flippers. In *46th AIAA Aerospace Sciences Meeting*, Reno, NV, Jan. 2008. AIAA Paper 2008-584.

[4]M.J. Mchenry and J. Jed. The ontogenetic scaling hydrodynamics and swimming performance in jellyfish (aurelia aurita). *Journal of Experimental Biology*, 206:4125–4137, 2003.

[5]O. Dabiry. On the estimation of swimming and flying forces from wake measurements. *Journal of Experimental Biology*, 208:3519–3532, 2005.

[6]J. Peng and O. Dabiri. A potential-flow, deformable-body model for fluid-structure interactions with compact vorticity: application to animal swimming measurements. *Exp. Fluids*, 43(2):655–664, 2007.

[7]H. Schlichting. *Boundary-Layer Theory*. McGraw-Hill, 7th edition, 1979.

[8]M. Lacroix and A. Garon. Numerical solution of phase change problems: an eulerian-lagrangian approach. *Numerical Heat Transfer, Part B*, 19:57–78, 1992.

[9]P. A. Sackinger, P. R. Schunk, and R. R. Rao. A newton-raphson pseudo-solid domain mapping technique for free and moving boundary problems: A finite element implementation. *Journal of Computational Physics*, 125:83–103, 1996.

[10]S. Etienne and D. Pelletier. A monolithic formulation for steady-state fluid-structure interaction problems. In 34^{th} *AIAA Fluid Dynamics Conference and Exhibit*, Portland, Oregon, June 2004. AIAA Paper 2004-2239.

[11]O. Schenk and K. Gärtner. Solving unsymmetric sparse systems of linear equations with pardiso. *Journal of Future Generation Computer Systems*, 20(3):475–487, 2004.

[12]O. Schenk and K. Gärtner. On fast factorization pivoting methods for symmetric indefinite systems. *Elec. Trans. Numer. Anal.*, 23:158–179, 2006.

[13]S. Etienne and D. Pelletier. Geometric conservation law and finite element methods for ale simulations of incompressible flow.

[14]S. Etienne, A. Hay, A. Garon, and D. Pelletier. Sensitivity analysis of unsteady fluid-structure interaction problems.

[15]S. Ichikawa and O. Mochizuki. Flow induced by a jellyfish. In *7th Offshore and Polar Engineering conference, Lisbon, Portugal*, 2007.